6406 *Macromolecules* **2009**, *42*, 6406–6413
DOI: 10.1021/ma9011076

Macromolecules
ARTICLE

# Synthesis and Degradation Behavior of Cyclic Poly(ε-caprolactone)

**Jessica N. Hoskins and Scott M. Grayson***

*Department of Chemistry, Tulane University, New Orleans, Louisiana 70118*

*Received May 21, 2009; Revised Manuscript Received July 7, 2009*

ABSTRACT: Narrow polydisersity cyclic poly(caprolactone) was synthesized by cyclization of linear α, ω-functionalized poly(caprolactone). The linear precursors were prepared via ring-opening polymerization from an azido-functionalized initiator, followed by end group modification to attach a terminal alkyne. Click coupling afforded the cyclic polymer in high yields and provided linear and cyclic poly(caprolactone) with exactly identical molecular weight distributions. The thermal and acid-catalyzed degradation of analogous linear and cyclic poly(caprolactone) samples were investigated to determine the effect of architecture.

## Introduction

Aliphatic polyesters, such as poly(lactide), poly(glycolide), and poly(ε-caprolactone), are attractive materials for medical applications due to their combination of biocompatibility and biodegradability. As a result, they have been explored extensively for use in a variety of medical devices, including prosthetics, dental implants, stents, degradable sutures, and drug delivery scaffolds.[1] To address this diversity of applications, many architectures of poly(ε-caprolactone) (PCL) have been investigated, including star polymers,[2−4] hyperbranched polymers,[5,6] and graft polymers.[7−10] However, the exploration of cyclic PCL structures has been somewhat limited as a result of difficulties in their preparation. Because small cyclic molecules (e.g., cyclodextrins and crown ethers) have been utilized to encapsulate Ångstrom scale guests, larger macrocycles with the appropriate functionality are expected to have similar interactions with larger guest molecules. In order to explore the applications of cyclic polymer hosts within biological systems, the preparation of well-defined biocompatible and biodegradable cyclic polyesters is of particular interest.

Historically, the synthesis of cyclic polymers has been accomplished using three contrasting techniques: the cyclization of linear polymers with a bifunctional coupling reagent, cyclization of linear polymers with complementary end groups, and cyclic ring expansion.[11] The cyclization of homodifunctional polymers with a difunctional coupling reagent requires high dilution, and inevitably yields a mixture of linear and cyclic products.[12−14] A diversity of cyclic ring expansion techniques have been explored including lactone ring-opening polymerization,[15−18] polyhomologation,[19] ring-opening metathesis polymerization,[20,21] or carbene catalyzed ring-opening polymerization;[22] however, these techniques frequently yield materials with high polydispersity and limited molecular weight control, as well as limited inclusion of backbone or side-chain functionality A final route, the cyclization of α,ω-heterodifunctional linear precursors, can provide the high cyclic purity, the high functional group tolerance, and the low polydispersity desired for a range of *in vivo* applications.[23]

Up until recently, the vast majority of routes for the preparation of cyclic PCL have utilized the cyclic ring expansion of lactones.[15−18] Kricheldorf and co-workers pioneered this approach by preparing macrocyclic PCL by the ring-opening polymerization of ε-caprolactone (εCL) using cyclic tin dialkoxides as the initiating species.[18] Though the resultant cyclic polymers were hydrolytically labile, end-capping with 1,3-dithian-2-one or UV irradiation of acrylate side chains provided more rugged cyclic PCL.[24,25] This technique was also utilized in the copolymerization of εCL and a functionalized monomer to allow attachment of poly(ethylene oxide) (PEO) grafts to create "sun-shaped" macrocycles.[25] In each of these studies, however, the polydispersity was somewhat broad (>1.4). While the α,ω-heterodifunctional cyclization route appears to be an attractive alternative for providing better-defined cyclic PCL this approach has not, to our knowledge, been applied previously to either ring-opening polymerizations or biodegradable polymers until recent explorations in our laboratories.[26]

An extremely versatile technique for the coupling of linear polymers[27,28] involves the use of the highly efficient and functional group tolerant Huisgen 1,3-dipolar cycloaddition "click" reaction.[29,30] The cyclization of α-alkynyl-ω-azido heterodifunctional polymers under high dilution has afforded nearly quantitative yields of polymer macrocycles prepared from linear atom transfer radical polymerization (ATRP) precursors including: polystyrene,[31] poly(*N*-isopropylacrylamide),[32] and copolymers of methyl acrylate and styrene.[33] More recently, this click approach has been applied to prepare cyclic poly(*N*-isopropyl acrylamide) and polystyrene using reversible addition−fragmentation chain transfer (RAFT) polymerization.[34,35] Herein we investigate the compatibility of this cyclization technique with the ring-opening polymerization (ROP) of caprolactone, as the "click" cyclization technique is expected to be sufficiently mild to preserve the ester linkages of the polymer backbone.[36,37]

In addition, because the degradability of PCL is one of its most attractive features, the topological effects on the kinetics of degradation are of particular interest. The cyclic architecture is expected to have a profound effect on the mechanisms of degradation, but these effects have yet to be studied, owing to the relative difficulty of preparing comparable sets of linear and cyclic structures using previous ring expansion techniques. The described ring closure technique provides unique access to linear and cyclic PCL samples with exactly identical average molecular weight and polydispersity, which are required to elucidate of the effect of the cyclic topology on degradation. Therefore, this study has also included the investigations of both thermal and hydrolytic degradation of the cyclic PCL and has compared those data with their exact linear analogs.

## Experimental Section

**Materials.** All reagents were purchased from Aldrich and used without further purification, unless otherwise noted. εCL

---

*Corresponding author. E-mail: sgrayson@tulane.edu.

**Scheme 1. Polymerization and Cyclization of Poly(ε-caprolactone)[a]**

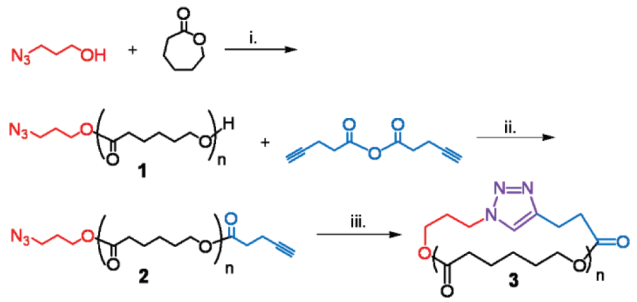

[a] (i) Tin(II) ethylhexanoate, 130 °C. (ii) 4-(Dimethylamino)pyridine, $CH_2Cl_2$, pyridine, 40 °C. (iii) $Cu^IBr$, *N*,*N*,*N*′,*N*″,*N*″-pentamethyldiethylene triamine (PMDETA), $CH_2Cl_2$.

was dried over calcium hydride at room temperature for at least 8 h and distilled under reduced pressure just prior to use. Copper(I) bromide (CuBr) was purified by washing with acetic acid. The 3-azidopropanol initiator was synthesized as reported in literature and dried over anhydrous $MgSO_4$ immediately prior to use.[38] The synthesis of 4-pentynoic anhydride was also synthesized according to previously published procedures.[39] All solvents were reagent grade and used without further distillation or purification.

**Nomenclature.** In order to simplify the identification of compounds, the following nomenclature was used: A prefix *l*- was assigned to linear polymers and *c*- to cyclic polymer and PCL was used as the abbreviation for poly(ε-caprolactone). $N_3-$ prefix was used to represent the 3-azidopropoxy initiating group, and a suffix was added to identify the functionality at the terminal end of the polymer chain: −OH for the terminal alcohol, −C≡CH for the terminal 4-pentynoic ester.

**Characterization.** All $^1H$ NMR (400 MHz) and $^{13}C$ NMR (100 MHz) were obtained using a Varian Mercury spectrometer (Palo Alto, CA), using TMS = 0.00 ppm for $^1H$ calibration. The integration data for the polymers repeat units is reported as multiples of "*n*" where *n* is the calculated degree of polymerization of the PCL as determined by NMR integration. The subscripts EG (end group) and RU (repeat unit) were used to aid in the clarity of NMR resonance assignments, and the particular assignment is designated by italicization.

Mass spectral data was acquired using a Bruker Autoflex III matrix-assisted laser desorption time-of-flight mass spectrometer (MALDI−TOF MS) with delayed extraction using both positive ion and reflector detection modes. For all PCL polymers, THF stock solutions of 9-nitroanthracene as the matrix (20 mg $mL^{-1}$) and NaI as the counterion (10 mg $mL^{-1}$) were used. The polymer sample was prepared at a 2 mg $mL^{-1}$ concentration in THF. MALDI samples were prepared by combining 50 μL of polymer solution, 100 μL of counterion solution, and 200 μL of matrix solution. For PCL < 10K: the pulsed ion extraction delay was set to 10 ns, with an ion source 1 voltage of 19.00 kV, an ion source 2 voltage of 16.55 kV, a lens voltage of 8.8 kV, a low mass gate at 750 AMU, and a laser power set to 45%. For PCL > 10K: the pulsed ion extraction delay was set to 30 ns, with an ion source 1 voltage of 19.00 kV, an ion source 2 voltage of 15.8 kV, a lens voltage of 8.3 kV, a low mass gate at 1000 amu, and a laser power set to 45%. The $M_n$ and PDI were calculated using PolyTools software.

**Table 1. Number Average Molecular Weight ($M_n$) and Polydispersity Index (PDI = $M_w/M_n$) Data for PCL Samples (1 = $N_3$-*l*-PCL−OH, 2 = $N_3$-*l*-PCL−C≡CH, 3 = *c*-PCL) of Six Different Molecular Weights (a−f)[c]**

| | $M_n$ | | | PDI | |
|---|---|---|---|---|---|
| Polymer | GPC[a] | GPC[b] | MALDI | GPC | MALDI |
| 1a | 6850 | 3380 | 3830 | 1.14 | 1.02 |
| 2a | 7440 | 3690 | 3860 | 1.20 | 1.02 |
| 3a | 4450 | 2130 | 3780 | 1.10 | 1.02 |
| 1b | 8940 | 4500 | 5120 | 1.14 | 1.03 |
| 2b | 9090 | 4580 | 5050 | 1.15 | 1.03 |
| 3b | 6440 | 3160 | 4940 | 1.13 | 1.03 |
| 1c | 11100 | 5670 | 6080 | 1.08 | 1.02 |
| 2c | 11700 | 6000 | 6220 | 1.08 | 1.02 |
| 3c | 7680 | 3820 | 6180 | 1.09 | 1.02 |
| 1d | 15800 | 8290 | 7440 | 1.09 | 1.02 |
| 2d | 17600 | 9300 | 7430 | 1.13 | 1.02 |
| 3d | 12400 | 6390 | 7840 | 1.07 | 1.02 |
| 1e | 21700 | 11600 | 11950 | 1.07 | 1.01 |
| 2e | 22800 | 11300 | 11930 | 1.08 | 1.01 |
| 3e | 17800 | 9400 | 12050 | 1.09 | 1.01 |
| 1f | 25200 | 13700 | 14900 | 1.09 | 1.01 |
| 2f | 25500 | 13800 | 15000 | 1.07 | 1.01 |
| 3f | 20300 | 10800 | 15000 | 1.08 | 1.01 |

[a] Calibrated based upon linear polystyrene standards. [b] Corrected value for PCL,[40] using $M_n(PCL)=0.259M_n(PS)^{1.073}$ [c] The data were calculated by gel permeation chromatography (GPC) and matrix-assisted laser desorption ionization (MALDI) mass spectrometry.

Size exclusion chromatography (SEC) was carried out on a Waters model 1515 series pump (Milford, MA) with three-column series from Polymer Laboratories, Inc. consisting of PLgel 5 μm Mixed D (300 mm × 7.5 mm, molecular weight range 200−400 000), PLgel 5 μm 500 Å (300 mm x 7.5 mm, molecular weight range 500−30,000), and PLgel 5 μm 50 Å (300 mm × 7.5 mm, molecular weight range up to 2000) columns. The system was fitted with a Model 2487 differential refractometer detector and anhydrous tetrahydrofuran was used as the mobile phase (1 mL $min^{-1}$ flow rate). The resulting molecular weight was based on calibration using linear polystyrene standards, and these apparent molecular weights were converted to absolute molecular weights for PCL using the previously reported conversion[40] $M_n(PCL) = 0.259 \times M_n(PS)^{1.073}$. Data were collected and processed using Precision Acquire software.

Differential scanning calorimetry (DSC) was performed on a TA Instruments Q200 thermal analysis system equipped with a liquid nitrogen cooling system in platinum pans from −70 to +100 °C with a heating/cooling rate of 10 °C per minute. Data was collected on the third heating/cooling cycle, with the $T_m$ calculated as the maximum of the endotherm. Enthalpy and temperature calibration were performed by heating a standard metal (indium) through its melting transition and extrapolating the observed heat of fusion and melting point to known values.

Thermogravimetric analysis (TGA) was performed on a TA Instruments TGA 2950 Thermogravimetic Analyzer in platinum pans from room temperature to 600 °C with a heating rate of 20 °C per minute and $N_2$ as the purge gas. Data was processed using TA Instruments Universal Analysis software.

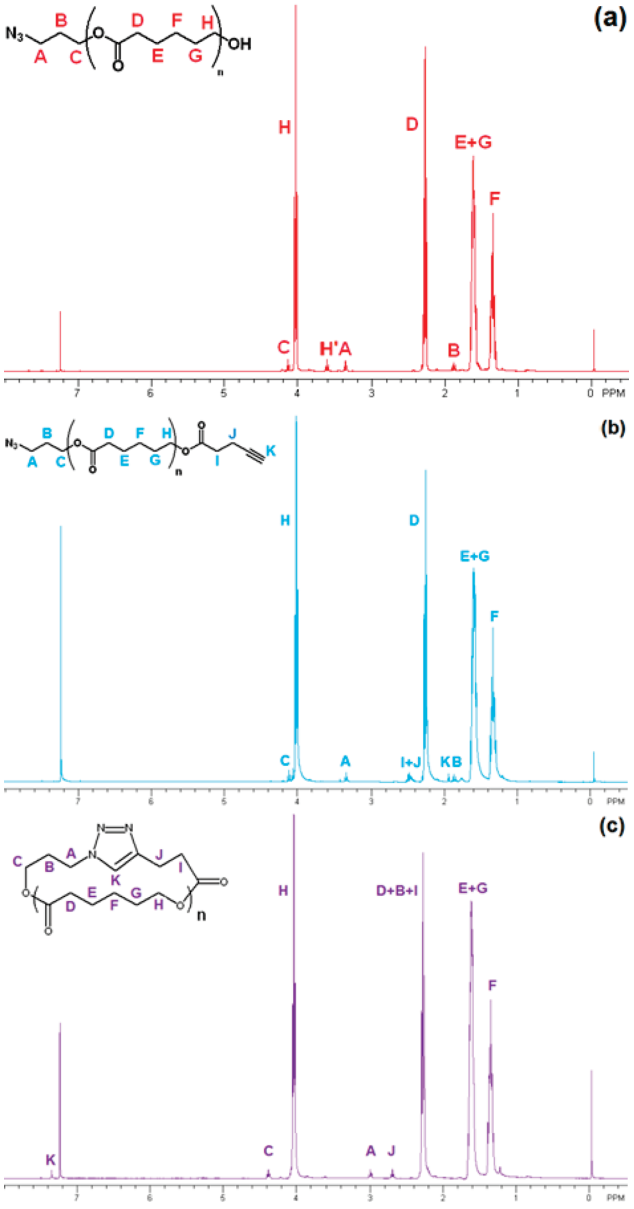

**Figure 1.** $^1$H NMR of PCL before esterification, (a) **1a**, before cyclization, (b) **2a**, and after click cyclization, (c) **3a**. The successful click reaction is highlighted by the appearance of the triazole proton (K in part c) and the disappearance of the terminal alkyne proton (K in part b).

**Synthesis of *l*-N$_3$−PCL−OH (1) (Scheme 1).** In a representative polymerization, 3-azidopropanol (0.108 g, 1.1 mmol) and εCL (26.9 g, 0.236 mol) were added through a rubber septum via syringe to a previously dried reaction vessel. Tin(II) ethylhexanoate (Sn(Oct)$_2$) (0.043 g, 0.1 mmol) was added to the reaction mixture via syringe, followed by immediate immersion of the reaction flask into an oil bath at 130 °C. At various time points (15, 20, 25, 30, 35, and 45 min), a 4 mL aliquot was removed via syringe and immediately diluted with dichloromethane, precipitated into a 1:1 mixure of hexanes and diethyl ether, recovered by filtration, and dried *in vacuo* prior to characterization. The variation in polymerization time produced a series of polymers with narrow polydispersities and average molecular weights from 4000 to 15 000. Representative characterization data follow. $^1$H NMR (CDCl$_3$, $\delta$, ppm): 1.31 (m, 2*n*, $(-\mathrm{CH_2CH_2C}H_2\mathrm{CH_2CH_2}-)_\mathrm{RU}$), 1.57 (m, 4*n*, $(-\mathrm{CH_2C}H_2\mathrm{CH_2C}H_2\mathrm{CH_2}-)_\mathrm{RU}$), 1.88 (m, 2, $J$ = 6.3 Hz, $(\mathrm{N_3CH_2C}H_2\mathrm{CH_2}-)_\mathrm{EG}$), 2.27 (t, 2*n*, $J$ = 7.6, $(-\mathrm{COC}H_2\mathrm{CH_2}-)_\mathrm{RU}$), 3.37 (t, 2, $J$ = 6.3, $(\mathrm{N_3C}H_2\mathrm{CH_2}-)_\mathrm{EG}$), 3.60 (t, 2, $J$ = 6.6 Hz, $(-\mathrm{CH_2C}H_2\mathrm{OH})_\mathrm{EG}$), 4.03 (t, 2*n*, $J$ = 6.3 Hz, $(-\mathrm{CH_2C}H_2\mathrm{OCO})_\mathrm{RU}$), 4.14 (t, 2, $J$ = 6.2 Hz, $(-\mathrm{N_3CH_2CH_2C}H_2\mathrm{OCO}-)_\mathrm{EG}$); calcd $M_\mathrm{n}$ = 4600. $^{13}$C NMR (CDCl$_3$, $\delta$, ppm): 24.78 $(-\mathrm{COCH_2}C\mathrm{H_2CH_2}-)_\mathrm{RU}$, 25.73 $(-\mathrm{CH_2CH_2}C\mathrm{H_2CH_2CH_2}-)_\mathrm{RU}$, 28.54 $(-\mathrm{CH_2}C\mathrm{H_2CH_2O}-)_\mathrm{RU}$, 34.32 $(-\mathrm{OCO}C\mathrm{H_2CH_2}-)_\mathrm{RU}$, 64.36 $(-\mathrm{CH_2}C\mathrm{H_2O}-)_\mathrm{RU}$, 173.79 $(-\mathrm{O}C\mathrm{OCH_2}-)_\mathrm{RU}$. MS (MALDI−TOF): (*m*/*z*), $M_\mathrm{n}$ = 3830; PDI = 1.02. SEC: $M_\mathrm{n}$ = 6850; PDI = 1.14.

**Preparation of *l*-N$_3$−PCL−C≡CH (2).** The polymer **1** (0.14 g, 8.4 × 10$^{-4}$ mol) was dissolved in 10 mL of pyridine. 4-Pentynoic anhydride (0.060 g, 4.4 × 10$^{-4}$ mol), 4-(dimethylamino)pyridine (3 mg, 2.1 × 10$^{-5}$ mol), and 10 mL of dichloromethane were added to the reaction flask. The reaction was stirred until MALDI−TOF monitoring indicated the reaction was complete (typically occurring after about 8 h). The crude reaction mixture was extracted three times from saturated aqueous NaHSO$_4$ and three times from saturated aqueous NaHCO$_3$ into dichloromethane. The organic layer was dried over anhydrous MgSO$_4$, filtered, and concentrated prior to precipitation from dichloromethane into cold methanol. The product was recovered by filtration and dried *in vacuo*. (Yield: 89%.) Representative characterization data follow. $^1$H NMR (CDCl$_3$, $\delta$, ppm): 1.33 (m, 2*n*, $(-\mathrm{CH_2CH_2C}H_2\mathrm{CH_2CH_2}-)_\mathrm{RU}$), 1.59 (m, 4n, $(-\mathrm{CH_2C}H_2\mathrm{CH_2C}H_2\mathrm{CH_2}-)_\mathrm{RU}$), 1.88 (m, 2, $(\mathrm{N_3CH_2C}H_2\mathrm{CH_2}-)_\mathrm{EG}$), 1.98 (s, 1, $(-\mathrm{CH_2CC}H)_\mathrm{EG}$), 2.27 (t, 2n, $(-\mathrm{COC}H_2\mathrm{CH_2}-)_\mathrm{RU}$), 2.45 (m, 4, $(-\mathrm{COC}H_2\mathrm{C}H_2\mathrm{CCH})_\mathrm{EG}$), 3.37 (t, 2, $(\mathrm{N_3C}H_2\mathrm{CH_2}-)_\mathrm{EG}$), 4.03 (t, 2n, $(-\mathrm{CH_2C}H_2\mathrm{OCO})_\mathrm{RU}$), 4.14 (t, 2, $(\mathrm{N_3CH_2CH_2C}H_2\mathrm{OCO}-)_\mathrm{EG}$); calcd $M_\mathrm{n}$ =4600. $^{13}$C NMR (CDCl$_3$, $\delta$, ppm): 24.78 $(-\mathrm{COCH_2}C\mathrm{H_2CH_2}-)_\mathrm{RU}$, 25.73 $(-\mathrm{CH_2CH_2}C\mathrm{H_2CH_2CH_2}-)_\mathrm{RU}$, 28.54 $(-\mathrm{CH_2}C\mathrm{H_2CH_2O}-)_\mathrm{RU}$, 34.32 $(-\mathrm{OCO}C\mathrm{H_2CH_2}-)_\mathrm{RU}$, 64.36 $(-\mathrm{CH_2}C\mathrm{H_2O}-)_\mathrm{RU}$, 173.79 $(-\mathrm{O}C\mathrm{OCH_2}-)_\mathrm{RU}$. MS (MALDI−TOF): (*m*/*z*), $M_\mathrm{n}$ = 3860; PDI = 1.02. SEC: $M_\mathrm{n}$ = 7440; PDI = 1.20.

**Synthesis of *c*-PCL (3).** A 0.22 mM solution of compound **2** in dichloromethane (50 mL) was degassed and backfilled with N$_2$ with two freeze, pump, thaw cycles. In a separate flask, *N*,*N*,*N*′,*N*″,*N*″-pentamethyldiethylenetriamine (PMDETA) (0.211 g, 1.2 mmol) was dissolved in dichloromethane (100 mL) and degassed with one freeze, pump, thaw cycle. Immediately following a second freeze, CuBr (0.159 g, 1.1 mmol) was added, followed by a pump and thaw cycle. Upon thawing, a syringe and syringe pump were used to transfer the solution of **2** to the rapidly stirring CuBr/PMDETA solution at a rate of 2 mL per hour. After complete addition of the polymer solution, the reaction mixture was allowed to stir for an additional 2 h and was then extracted three times from saturated aqueous NaHSO$_4$ into dichloromethane. The organic layer was dried over anhydrous MgSO$_4$, filtered, and concentrated prior to precipitation from dichloromethane into a 1:1 mixture of chilled hexanes and diethyl ether. The product was isolated via filtration and dried *in vacuo*. (Yield: 57%.) Representative characterization data follow. $^1$H NMR (CDCl$_3$, $\delta$, ppm): 1.33 (m, 2*n*, $(-\mathrm{CH_2CH_2C}H_2\mathrm{CH_2CH_2}-)_\mathrm{RU}$), 1.59 (m, 4*n*, $(-\mathrm{CH_2C}H_2\mathrm{CH_2C}H_2\mathrm{CH_2}-)_\mathrm{RU}$), 2.27 (t, 4*n*, $(-\mathrm{COC}H_2\mathrm{CH_2}-)_\mathrm{RU}$), $(-\mathrm{CH_2C}H_2\mathrm{CH_2}-\mathrm{N_{triazole}})$, $(\mathrm{C_{triazole}}-\mathrm{CH_2C}H_2\mathrm{CO}-))$, 2.70 (m, 4, $(\mathrm{C_{triazole}}-\mathrm{C}H_2\mathrm{CH_2}-))$, 3.00 (t, 2. $(-\mathrm{CH_2C}H_2\mathrm{N_{triazole}}-))$, 4.03 (t, 2n, $(-\mathrm{CH_2C}H_2\mathrm{OCO})_\mathrm{RU}$), 4.38 (t, 2, $(-\mathrm{OC}H_2\mathrm{CH_2CH_2}-\mathrm{N_{triazole}}-))$, 7.35 (s, 1, $(-\mathrm{NC}H\mathrm{C}-))$; calcd $M_\mathrm{n}$ =4600. $^{13}$C NMR (CDCl$_3$, $\delta$, ppm): 24.78 $(-\mathrm{COCH_2}C\mathrm{H_2CH_2}-)_\mathrm{RU}$, 25.73 $(-\mathrm{CH_2CH_2}C\mathrm{H_2CH_2CH_2}-)_\mathrm{RU}$, 28.54 $(-\mathrm{CH_2}C\mathrm{H_2CH_2O}-)_\mathrm{RU}$, 34.32 $(-\mathrm{OCO}C\mathrm{H_2CH_2}-)_\mathrm{RU}$, 64.36 $(-\mathrm{CH_2}C\mathrm{H_2O}-)_\mathrm{RU}$, 173.79 $(-\mathrm{O}C\mathrm{OCH_2}-)_\mathrm{RU}$. MS (MALDI−TOF): (*m*/*z*), $M_\mathrm{n}$ = 3780; PDI = 1.02. SEC: $M_\mathrm{n}$ = 4450; PDI = 1.10.

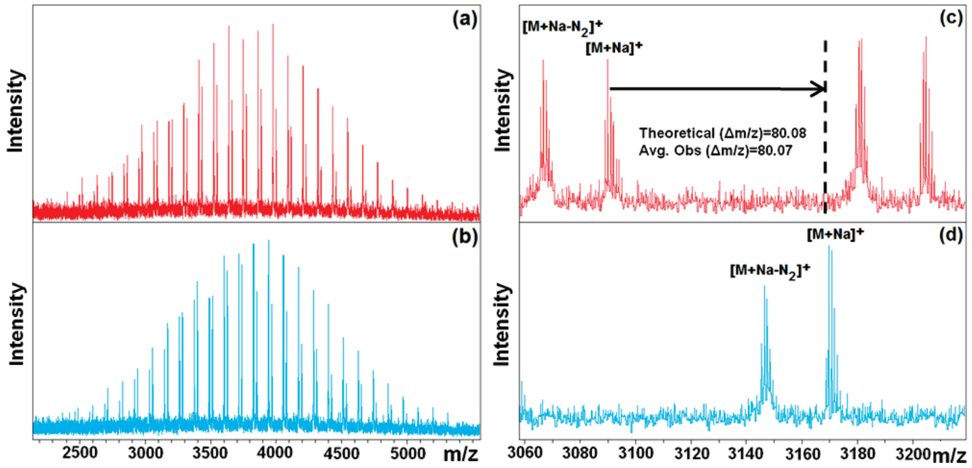

**Figure 2.** MALDI−TOF MS spectra of (a) *l*-$N_3$−PCL−OH, **1a** and (b) *l*-$N_3$−PCL−C≡CH, **2a**. (c and d) Spectra of **1a** and **2a** respectively, but with the spectra expanded in the region from 3060 to 3200 *m*/*z*.

**Hydrolytic Degradation of *l*-$N_3$−PCL−C≡CH and *c*-PCL.** The PCL sample (0.026 g, $4.4 \times 10^{-6}$ mol) was dissolved in mixture of 6.75 mL of dichloromethane and 1.5 mL of methanol in a scintillation vial. Then p-toluenesulfonic acid (p-TSA) (0.0142 g, $8.25 \times 10^{-5}$ mol) was added to the reaction mixture, to produce a solution 0.01 M in p-TSA. The vial was capped and the contents stirred at room temperature. At a series of time points (3, 6, 12, 24, 48, 96, and 192 h), a 1 mL sample was removed via syringe. This sample was quenched by extraction with saturated aqueous $NaHCO_3$, followed by evaporation of the organic layer and thorough drying *in vacuo*. The samples were dissolved in THF just prior to characterization in order to minimize possible self-catalyzed degradation. MALDI−TOF MS number average molecular weight ($M_n$) and polydispersity data was determined by the weighted averaging of the distributions of each of the various degradation products, utilizing the PolyTools software. SEC $M_n$ and PDI data was determined by integrating over the entire distribution of peaks in the Precision Acquire software, calibrated against linear polystyrene standards. This procedure was repeated in triplicate.

## Results and Discussion

**Synthesis of Linear PCL Precursors.** The strategy for preparing well-defined cyclic PCL involves the initial preparation of well-defined α, ω-heterodifunctional linear precursors with complementary click coupling functionalities. These were prepared by polymerization of εCL from an azido functionalized initiator followed by the postpolymerization coupling of a complementary alkyne group. Using 3-azidopropanol as the initiator,[38] εCL was polymerized in bulk with tin(II) ethylhexanoate ($Sn(Oct)_2$) as catalyst at 130 °C (Scheme 1). Six samples of the azide/alcohol terminated PCL, **1**, ($N_3$-*l*-PCL−OH) were prepared with average molecular weights ranging from 4000 to 15 000. After purification by precipitation, the polymers were characterized by MALDI−TOF MS, SEC, and NMR (Table 1).

Size exclusion chromatography verified the narrow polydispersity (PDI ≤ 1.20) of the PCL samples **1a**−**1f**, with the higher molecular weights (**1c**−**1f**) demonstrating PDIs below 1.10 (Table 1). Because the $M_n$ data was calibrated against polystyrene standards, the raw data over predicts the molecular weight, but application of the previously reported conversion factor yielded data that was in close agreement with other mass determination techniques. $^1$H and $^{13}$C NMR data analysis exhibited the expected resonances, $\delta = 1.31$, $\delta = 1.57$, $\delta = 2.27$, and $\delta = 4.03$ ppm (F, E and G, D, and H in Figure 1a), corresponding to the protons along the polymer backbone. The weak resonance at $\delta = 3.60$ ppm corresponds to the methylene immediately adjacent to the terminal hydroxyl group (H′ in Figure 1a). For lower molecular weights, the weak resonances that correspond to the azido-functionalized end group at $\delta = 1.88$, $\delta = 3.37$, and $\delta = 4.14$ ppm (B, A, and C in Figure 1a) can be clearly integrated to provide molecular weight calculations comparable to those obtained from the SEC chromatograms and mass spectra. Because of the high precision of the obtained MALDI−TOF mass spectral data, detailed structural analysis could be performed across the range of molecular

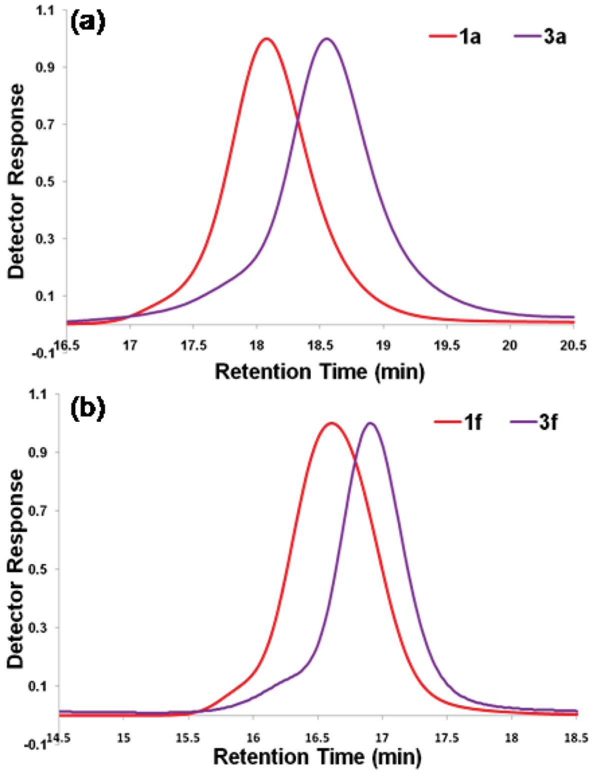

**Figure 3.** GPC spectra of linear and cyclic PCL, (a) **1a** and **3a**, (b) **1f** and **3f**, respectively, showing the shift in retention time of the cyclic polymer due to the smaller hydrodynamic volume.

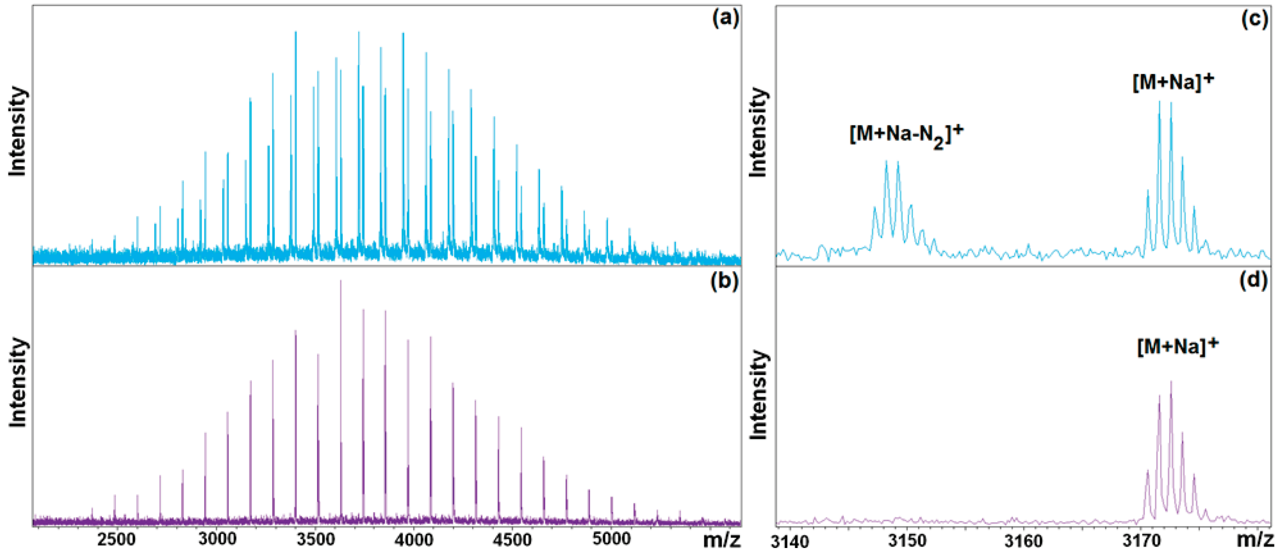

**Figure 4.** MALDI−TOF mass spectra of (a) *l*-$N_3$−PCL-C≡CH, **2a** and (b) *c*-PCL, **3a**. (c) and (d) correspond to **2a** and **3a** respectively, but with the spectra expanded in the region from 3140 to 3180 *m*/*z*. The MALDI−TOF mass spectra confirm that no change in average molecular weight occurs during the cyclization reaction.

weights investigated. The mass spectra were obtained using 9-nitroanthracene as a matrix and sodium iodide as the cation source in reflector mode. The resulting spectra exhibited two distinct molecular weight distributions with nearly identical $M_n$, but a mass offset of approximately 23 Da (Figure 2a). By varying the counterion (e.g., $K^+$, $Ag^+$) it was apparent that the higher molecular weight distribution corresponded to the $[M + \text{cation}]^+$ ion, with the observed molecular weights values within 0.06 D of the theoretical exact molecular weights. The resolution of the slightly lower mass distribution was significantly reduced, suggesting that it may be the result of a metastable decaying ion. This hypothesis was further supported by the drifting mass difference between the two distributions (23.03 Da at low mass and 23.63 Da at high mass) which occurs in reflector mode if the ion decays during the flight path. As expected, altering the detection to linear mode resulted in significant reduction in the signal intensity of the second distribution, and refocused of the mass difference to approximately 28 ± 1 Da. As a result, the authors are convinced that this second distribution[41] results from the postsource expulsion of $N_2$ gas from the ionized polymer sample. Such decay is frequently observed in the mass spectra of small molecule azides, and often represent the base peak of the mass spectra.[42,43] The observation of only these two mass distributions ($[M + Na]^+$ and $[M + Na - N_2]^+$) suggests that the polymer initiated exclusively from the azide functionalized alcohol.

The reaction of the hydroxyl end group of the $N_3$-*l*-PCL−OH, **1**, with pentynoic anhydride yielded the desired linear PCL precursor, $N_3$-*l*-PCL−C≡CH, **2**, with complementary click functionalities on opposite ends. GPC analysis verified that while the mass did not shift noticeably, the narrow polydispersity was maintained during this transformation (Table 1). $^1$H NMR analysis revealed loss of the free hydroxyl and the shift of the adjacent methylene at $\delta = 3.60$ ppm resonance to $\delta = 4.03$ ppm (H′ in Figure 1, parts a and b) corresponding to the ester methylene. In addition, new resonances corresponding to the pentynoic group were seen at $\delta = 2.45$ ppm (I and J) and $\delta = 1.98$ ppm (K, Figure1b). The ability to verify this transformation, however, was limited at molecular weights above 7000 because of the low signal for the end groups. However, MALDI−TOF MS mass spectral analysis did provided convincing evidence of a quantitative esterification even at higher molecular weights. Both the $[M + Na]^+$ and the $[M + Na - N_2]^+$ distributions demonstrated a shift in the mass spectra during the conversion of **1** to **2** to a slightly higher molecular weight, and no trace of unreacted starting material could be observed in the MALDI−TOF mass spectra (Figure 2b). The average mass shift across the entire mass distribution from the hydroxyl precursor, **1**, to the esterified product, **2**, was determined to be 80.07 ± 0.15 Da, which corresponds closely to the theoretical value for the addition of the pentynoic ester, 80.08.

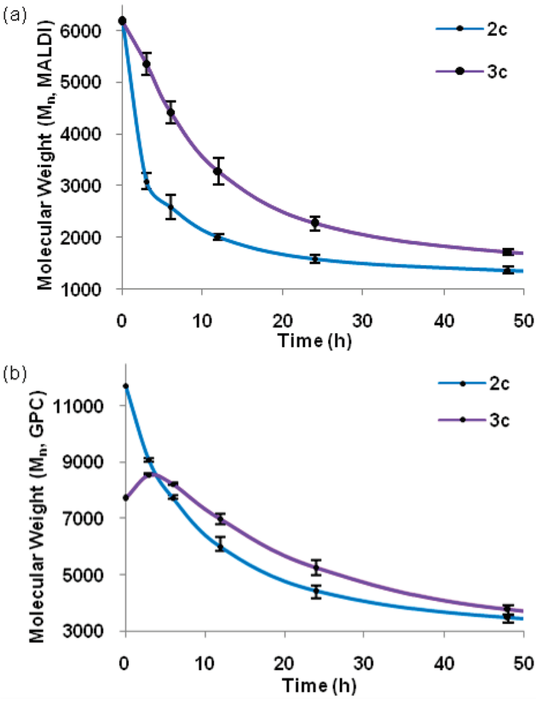

**Figure 5.** Comparison of observed number average molecular weight ($M_n$) during controlled hydrolytic degradation of cyclic and linear PCL as a function of time as measured by (a) MALDI−**TOF MS and** (**b**) **GPC.**

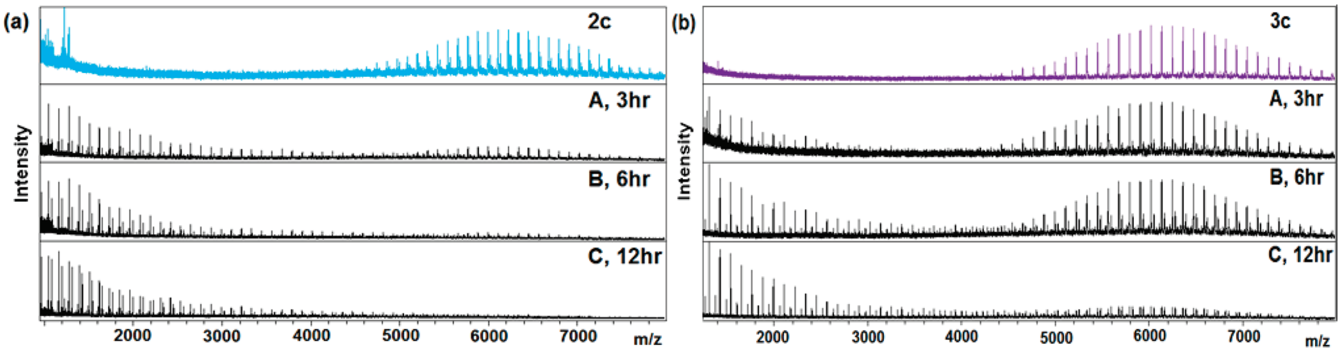

**Figure 6.** MALDI TOF spectra of (a) linear PCL, **2c**, and (b) cyclic PCL, **3c**, and the spectra of the hydrolytic degradation products at the first three time points: 3 (A), 6 (B), and 12 h (C).

**Cyclization of the Linear PCL Precursors.** The continuous addition "click" polymer cyclization technique was then employed to cyclize **2**.[31] This technique utilizes the fact that $\alpha,\omega$-functionalized polymers will favor intramolecular cyclization under extremely dilute Ruggli-Ziegler conditions.[44,45] In order to avoid the need for vast quantities of solvent, a dilute solution of the $N_3$-*l*-PCL−≡ linear precursor (0.22 mM) was added dropwise via a syringe pump to the solution of copper catalyst at a rate (2 mL/min) slower than the click reaction, to ensure high dilution of the linear precursor throughout the course of the reaction.[46] The characteristic increase in the SEC retention time of the cyclic PCL, **3**, compared to its linear precursor, **2**, was used to confirm cyclization, as cyclic confinement leads to a reduced size in solution and therefore a slower elution (Table 1, Figure 3). For the lower molecular weight samples ($M_n$ = 3800), the formation of the "click" product, **3**, can also be observed by $^1$H NMR, as the alkyne proton resonance at about $\delta$ = 2.0 ppm disappears (K in Figure 1b), while a single proton resonance appears at about $\delta$ = 7.4 ppm (K in Figure 1c), corresponding to the proton on the triazole. Furthermore, a shift in the proton resonances immediately adjacent to the triazole is observed, from $\delta$ = 2.45 ppm and $\delta$ = 3.37 ppm to $\delta$ = 2.70 and $\delta$ = 3.00 ppm respectively (J and A in Figure 1b and 1c). A shift in the proton resonances two or three carbons removed from the triazole is observed as well (B, C, and I in Figure 1b and 1c). Furthermore, the MALDI−TOF MS spectra clearly retains the $[M + Na]^+$ distribution after cyclization because there is no weight loss or gain corresponding to the click cycloaddition (Figure 4); however, the $[M - N_2 + Na]^+$ distribution vanishes, as would be expected because the stable aromatic triazole product is no longer susceptible to the proposed loss of $N_2$.

**Hydrolytic Degradation of Linear and Cyclic PCL.** As the cyclization of linear precursors allows access to exactly analogous linear and cyclic architectures, the effect of this topological change on the polymers' physical properties can be easily measured. The degradation of analogous linear and cyclic PCL was compared using *p*-toluenesulfonic acid as transesterification catalyst in a mixture of 1:4.5 methanol/dichloromethane. Samples were removed at regular time intervals and characterized by MALDI−TOF MS and SEC (Figure 5). As expected, when the degradation was monitored by MALDI−TOF MS, the linear PCL exhibited a decreasing $M_n$ with an continuously decreasing slope with respect to time,[47,48] while the cyclic PCL demonstrated a significant lag in the reduction of the average molecular weight (and an inflection point) because the first ester cleavage in each chain changes the polymer topology, but does not result in a loss of mass (Figure 6). Monitoring the degradation by SEC showed a similar degradation trend for the linear PCL; however, the cyclic degradation exhibited an initial increase in molecular size as the PDI broadens, because the first cleavage opens up the cyclic polymer into a linear configuration, which displays a larger size in solution than the parent cyclic (Figure 7). However, after the first 12 h, when the majority of the polymer rings have been broken into linear fragments, the subsequent degradation follows a trend similar to that observed for the linear samples.[48]

**Thermal Characterization and Degradation of Linear and Cyclic PCL.** Thermal characterization of the cyclic PCL verifies the expected decrease in glass transition temperature when compared to linear analogs, as determined by DSC.[49,50] As a representative example, the linear PCL with an $M_n$ of 15 000 exhibited a $T_m$ transition at 59.1 °C, while the $T_m$ temperature for the cyclic analog was observed at 55.5 °C (see Supporting Information). In addition, the thermal degradation properties of analogous linear and cyclic PCL architectures, **1b**, **2b** and **3b** and **1f**, **2f** and **3f**, were studied using thermogravimetric analysis. The alcohol terminated samples exhibited a major inflection point in the degradation curve, around 490 °C, with a shoulder near 420 °C (see Supporting Information). The existence of two major degradation events is in agreement with the results reported for linear PCL by DuBois and co-workers[51] which they attribute to competing backbiting, and nonbackbiting degradations. The alkyne/azide terminated PCL samples, however, demonstrated a single well-defined inflection point around 500 °C, suggesting that the end-capping prevented backbiting depolymerization to regenerate caprolactone. Interestingly, the cyclic polymers thermal degradation pattern seemed nearly identical to the end-capped linear precursors, suggesting that the cyclic topology does not have a significant effect on thermal degradation.[52]

## Conclusion

The synthesis of well-defined cyclic PCL is possible by a combination of tin(II) ethylhexanoate catalyzed ring-opening polymerization and "click" coupling of the $\alpha$-azido,$\omega$-ethynyl-functionalized polymer. The Lewis acid catalyzed ring-opening polymerization yields a polymer with sufficiently narrow polydispersity to allow *in vivo* use, while the mild "click" cyclization has been proven to be compatible with the ester backbone. This method provides a synthetic route to analogous linear and cyclic PCL, and allows for the first time direct comparison of differing properties of PCL that result specifically from the differing topologies. As predicted, the cyclic architectures yield a delay in the molecular weight loss during the acid-catalyzed degradation as compared to their linear analogs, but the thermal degradation appears to be affected very little by the cyclization. The degradation behavior of cyclic PCL is of particular interest in

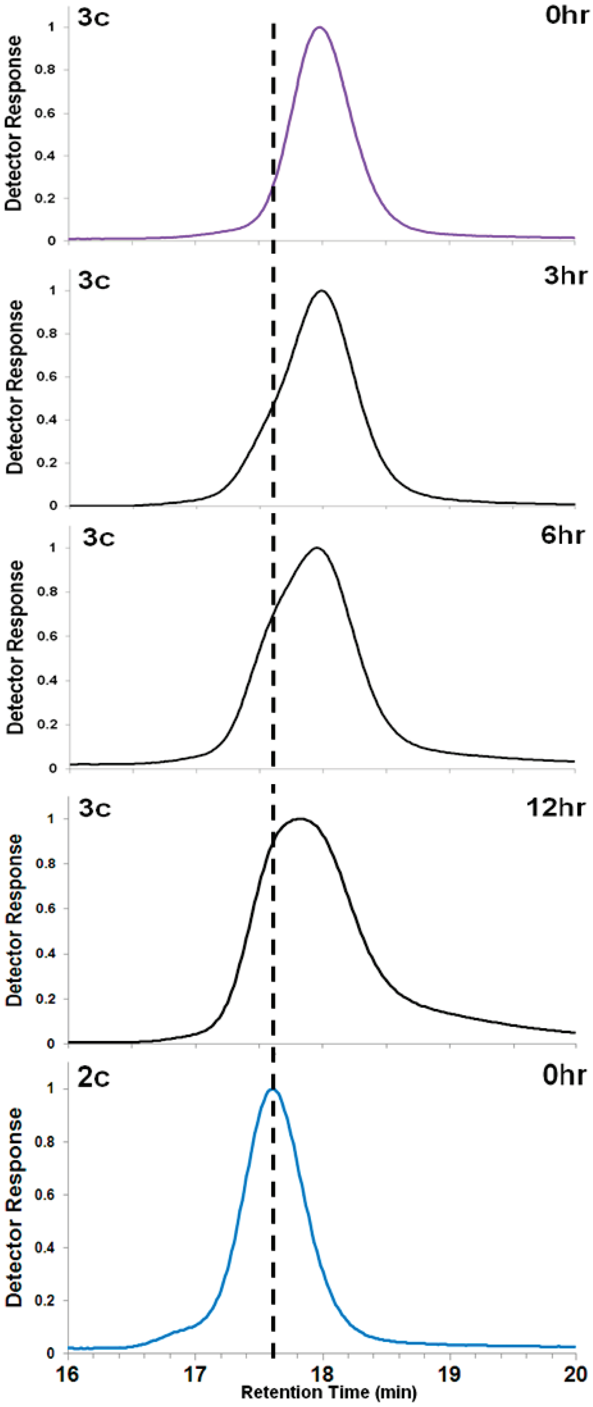

**Figure 7.** SEC traces of linear (**2c**) and cyclic (**3c**) PCL and the hydrolytic degradation products of the cyclic PCL at the first three time points: 3, 6, and 12 h. The cyclic architecture opens into its linear form (**2c**), initially shifting the distribution to a shorter retention time.

light of recent reports that the biodistribution of cyclic polyesters varies from their linear analogs.[53] Therefore, the degradation of cyclic polymeric carriers into their linear byproducts might be used as a stimulus-responsive control for drug targeting and eventual clearance of the carrier *in vivo*. Further investigations of the effect of the cyclic topology on a polymer's physical properties are continuing in our laboratory.

**Acknowledgment.** The authors acknowledge the donors of the Petroleum Research Fund, administered by the American Chemical Society (47108-G7), and Tulane University for financial support, the Louisiana Board of Regents for a Graduate Fellowship (J.N.H.), the NSF-MRI (0619770) for enabling MALDI−TOF mass spectral characterization, and the assistance from Michael Drenski and support from the Tulane Institute for Macromolecular Engineering and Science (NASA: NNC06AA18A) for thermal characterization. The authors also thank Dr. John Wiley and the University of New Orleans for graciously allowing DSC characterization of these polymers, and Prof. Dubois from the University of Mons-Hainaut for helpful discussions.

**Supporting Information Available:** Figures plotting raw MALDI−TOF MS, GPC, TGA and DSC data. This material is available free of charge via the Internet at http://pubs.acs.org.

## References and Notes

(1) Albertsson, A. C.; Varma, I. K. *Biomacromolecules* **2003**, *4*, 1466–1486.
(2) Trollsås, M.; Hedrick, J. L.; Mecerreyes, D.; Dubois, Ph.; Jérôme, R.; Ihre, H.; Hult, A. *Macromolecules* **1997**, *30*, 8508–8511.
(3) Hedrick, J. L.; Trollsås, M.; Hawker, C. J.; Atthoff, B.; Claesson, H.; Heise, A.; Miller, R. D.; Mecerreyes, D.; Jérôme, R.; Dubois, Ph. *Macromolecules* **1998**, *31*, 8691–8705.
(4) Hecht, S.; Ihre, H.; Fréchet, J. M. J. *J. Am. Chem. Soc.* **1999**, *121*, 9239–9240. (d) Corbin, P. S.; Webb, M. P.; McAlvin, J. E.; Fraser, C. L. *Biomacromolecules* **2001**, *2*, 223–232.
(5) Trollsås, M.; Atthoff, B.; Claesson, H.; Hedrick, J. L. *Macromolecules* **1998**, *31*, 3439–3445.
(6) Liu, M.; Vladimov, N.; Fréchet, J. M. J. *Macromolecules* **1999**, *32*, 6881–6884. (c) Choi, J.; Kwak, S.-Y. *Environ. Sci. Technol.* **2007**, *41*, 3763–3768.
(7) Chung, T. C.; Rhubright, D. *Macromolecules* **1994**, *27*, 1313–1319.
(8) Choi, E.-J.; Kim, C.-H.; Park, J.-K. *Macromolecules* **1999**, *32*, 7402–7408.
(9) Gref, R.; Rodrigues, J.; Couvreur, P. *Macromolecules* **2002**, *35*, 9861–9867.
(10) Wiltshire, J. T.; Qiao, G. G. *Macromolecules* **2006**, *39*, 4282–4285.
(11) Laurent, B. A.; Grayson, S. M. *Chem. Soc. Rev.* **2009**, *38*, 2202−2213.
(12) Geiser, D.; Höcker, H. *Polym. Bull.* **1980**, *2*, 591–597.
(13) Roovers, J.; Toporowski, P. M. *Macromolecules* **1983**, *16*, 843–849.
(14) Hadjichristidis, N.; Pitsikalis, M.; Pispas, S.; Iatrou, H. *Chem. Rev.* **2001**, *101*, 3747–3792.
(15) Hultzsch, K. C.; Spaniol, T. P.; Okuda, J. *Organometallics* **1997**, *16*, 4845–4856.
(16) Dyer, H. E.; Huijser, S.; Schwarz, A. D.; Wang, C.; Duchateau, R.; Mountford, P. *Dalton Trans.* **2008**, 32–35.
(17) Willans, C. E.; Sinenkov, M. A.; Fukin, G. K.; Sheridan, K.; Lynam, J. M.; Trifonov, A. A.; Kerton, F. M. *Dalton Trans.* **2008**, 3592–3598.
(18) Kricheldorf, H. R. *J. Polym. Sci., Polym. Chem.* **2004**, *42*, 4723–4742.
(19) Shea, K. J.; Lee, S. Y.; Busch, B. B. *J. Org. Chem.* **1998**, *63*, 5746–5747.
(20) Bielawski, C. W.; Benitez, D.; Grubbs, R. H. *J. Am. Chem. Soc.* **2003**, *125*, 8424–8425.
(21) Bielawski, C. W.; Benitez, D.; Grubbs, R. H. *Science* **2002**, *297*, 2041–2044.
(22) Culkin, D. A.; Jeong, W.; Csihony, S.; Gomez, E. D.; Balsara, N. P.; Hedrick, J. L.; Waymouth, R. M. *Angew. Chem., Int. Ed.* **2007**, *46*, 2627–2630.
(23) Schappacher, M.; Deffieux, A. *Macromolecules* **2001**, *34*, 5827–5832.
(24) Kricheldorf, H. R.; Lee, S. R.; Schittenhelm, N. *Macromol. Chem. Phys.* **1998**, *199*, 273–282.
(25) Li, H.; Jérôme, R.; Lecomte, P. *Macromolecules* **2008**, *41*, 650–654.
(26) Hoskins, J. N.; Grayson, S. M. *PMSE Prepr.* **2008**, *98*, 480–481.
(27) Tsarevsky, N. V.; Sumerlin, B. S.; Matyjaszewski, K. *Macromolecules* **2005**, *38*, 3558–3561.
(28) Gao, H.; Matyjaszewski, K. *J. Am. Chem. Soc.* **2007**, *129*, 6633–6639.
(29) Kolb, H. C.; Finn, M. G.; Sharpless, K. B. *Angew. Chem., Int. Ed.* **2001**, *40*, 2004–2021.
(30) Tornøe, C. W.; Christensen, C.; Meldal, M. *J. Org. Chem.* **2002**, *67*, 3057–3064.

(31) Laurent, B. A.; Grayson, S. M. *J. Am. Chem. Soc.* **2006**, *13*, 4238–4239.
(32) Xu, J.; Ye, J.; Lui, S. Y. *Macromolecules* **2007**, *40*, 9103–9110.
(33) Eugene, D. M; Grayson, S. M. *Macromolecules* **2008**, *41*, 5082–5084.
(34) Qiu, X. P.; Tanaka, F.; Winnik, F. M. *Macromolecules* **2007**, *40*, 7069–7071.
(35) Goldmann, A. S.; Quémener, D.; Millard, P. E.; Davis, T. P.; Stenzel, M. H.; Barner-Kowollik, C.; Muller, A. H. *Polymer* **2008**, *49*, 2274–2281.
(36) Joralemon, M. J.; O'Reilly, R. K.; Matson, J. B.; Nugent, A. K.; Hawker, C. J.; Wooley, K. L. *Macromolecules* **2005**, *38*, 5436–5443.
(37) Parrish, B.; Breitenkamp, R. B.; Emrick, T. *J. Am. Chem. Soc.* **2005**, *127*, 7404–7410.
(38) Mantovani, G.; Ladmiral, V.; Tao, L.; Haddleton, D. M. *Chem. Commun.* **2005**, 2089–2091.
(39) Malkoch, M.; Schleicher, K.; Drockenmuller, E.; Hawker, C. J.; Russell, T. P.; Wu, P.; Fokin, V. V. *Macromolecules* **2005**, *38*, 3663–3678.
(40) Dubois, P.; Barakat, I.; Jérôme, R.; Teyssie, Ph. *Macromolecules* **1993**, *23*, 4407–4412.
(41) Note: This metastable ion has been misreported as $[M + H]^+$ in some of the previous literature on polymer azides.
(42) Oliveira, A. M.; Barros, M. T.; Martins, A. M.; Cabral, M. A.; Dias, A. A.; Costa, M. L.; Cabral, M. H.; Moutinho, A. M.; Jennings, K. R. *Rapid Commun. Mass Spectrom.* **1999**, *13*, 559–51.
(43) Dinya, Z.; Benke, P.; Gyorgydeak, Z.; Somsak, L.; Jeko, J.; Pinter, I.; Kuszman, J.; Praly, J.-P. *J. Mass Spectrom.* **2001**, *36*, 211–219.
(44) Ruggli, P. *Leibigs Ann. Chem.* **1912**, *392*, 92–100.
(45) Ziegler, K. *Chem. Ber.* **1934**, 139–148.
(46) Harth, E.; van Horn, B.; Lee, V. Y.; Germack, D. S.; Gonzales, C. P.; Miller, R. D.; Hawker, C. J. *J. Am. Chem. Soc.* **2002**, *124*, 8652–8660.
(47) Fields, R. D.; Rodruguez, F.; Finn, R. K. *J. Appl. Polym. Sci.* **1974**, *18*, 3571–3579.
(48) Pitt, C. G.; Chasalow, F. I.; Hibionada, Y. M.; Klimas, D. M.; Schindler, A. *J. Appl. Polym. Sci.* **1981**, *26*, 3779–3787.
(49) Di Marzio, E. A.; Guttman, C. M. *Macromolecules* **1987**, *20*, 1403–1407.
(50) Gan, Y.; Dong, D.; Hogen-Esch, T. E. *Macromolecules* **1995**, *28*, 383–385.
(51) Persenaire, O.; Alexandre, M.; Degee, P.; Dubois, P. *Biomacromolecules* **2001**, *2*, 288–294.
(52) While the observed temperatures of degradation were about 80 degrees higher than those reported by Persenaire et al.,[29] poly(ethylene glycol) and polystyrene polymer standards were offset by a similar amount, suggesting the temperature offset results from variations due to heating rate and instrumentation.
(53) Nasongkla, N.; Chen, B.; Macaraeg, N.; Fox, M. E.; Fréchet, J. M. J.; Szoka, F. C. *J. Am. Chem. Soc.* **2009**, *131*, 3842–3843.